



HHS Public Access

Author manuscript

IEEE Trans Ultrason Ferroelectr Freq Control. Author manuscript; available in PMC 2015 May 13.

Published in final edited form as:

IEEE Trans Ultrason Ferroelectr Freq Control. 2015 May ; 62(5): 896–904. doi:10.1109/TUFFC.2015.7001.

Removal of Residual Cavitation Nuclei to Enhance Histotripsy Erosion of Model Urinary Stones

Alexander P. Duryea¹, William W. Roberts^{1,2}, Charles A. Cain¹, and Timothy L. Hall¹

¹Department of Biomedical Engineering, University of Michigan, Ann Arbor, MI, USA

²Department of Urology, University of Michigan, Ann Arbor, MI, USA

Abstract

Histotripsy has been shown to be an effective treatment for model kidney stones, eroding their surface to tiny particulate debris via a cavitation bubble cloud. However, similar to shock wave lithotripsy, histotripsy stone treatments display a rate-dependent efficacy with pulses applied at low rate generating more efficient stone erosion in comparison to those applied at high rate. This is hypothesized to be the result of residual cavitation bubble nuclei generated by bubble cloud collapse. While the histotripsy bubble cloud only lasts on the order of 100 μ s, these microscopic remnant bubbles can persist on the order of 1 second—inducing direct attenuation of subsequent histotripsy pulses and influencing bubble cloud dynamics. In an effort to mitigate these effects, we have developed a novel strategy to actively remove residual cavitation nuclei from the field using low-amplitude ultrasound pulses. Previous work has demonstrated that with selection of the appropriate acoustic parameters these bubble removal pulses can stimulate the aggregation and subsequent coalescence of microscopic bubble nuclei—effectively deleting them from the target volume. Here, we incorporate bubble removal pulses in histotripsy treatment of model kidney stones. It was found that when histotripsy is applied at low rate (1 Hz), bubble removal does not produce a statistically significant change in erosion. At higher pulse rates of 10, 100, and 500 Hz, incorporating bubble removal results in 3.7-, 7.5-, and 2.7-fold increases in stone erosion, respectively. High speed imaging indicates that the introduction of bubble removal pulses allows bubble cloud dynamics resulting from high pulse rates to more closely approximate those generated at the low rate of 1 Hz. These results corroborate previous work in the field of shock wave lithotripsy regarding the ill-effects of residual bubble nuclei, and suggest that high treatment efficiency can be recovered at high pulse rates through appropriate manipulation of the cavitation environment surrounding the stone.

INTRODUCTION

Previous work has documented that very-short, high-intensity ultrasound pulses applied at low duty cycle (histotripsy) can effectively erode model urinary stones via a cavitation bubble cloud localized on the stone surface [1–3]. In contrast to shock wave lithotripsy (SWL)—in which a stone is progressively comminuted, first into large pieces and then to

DISCLOSURE

W.W. Roberts, C.A. Cain, and T.L. Hall have financial interests and/or other relationships with HistoSonics, Inc., which has licensed intellectual property related to this manuscript.

fragments of decreasing size [4]—debris resulting from histotripsy erosion is composed of tiny particulate dust from the onset of treatment [1–3]. Furthermore, because histotripsy stone treatment is a surface erosion phenomenon, the rate of erosion is dependent on the exposed stone surface area [3, 5]. These facts lend themselves to a natural synergism between SWL and histotripsy stone treatments, as fragments generated by SWL can be rapidly eroded to fine debris via histotripsy pulses after initial stone subdivision is achieved [3].

While histotripsy offers a promising adjunct to traditional SWL stone treatments, much room is available for the optimization of histotripsy pulse sequences for the application of stone erosion. Indeed, previous work has indicated that histotripsy stone erosion displays a rate-dependent efficacy, with histotripsy applied at low pulse repetition frequency (PRF) producing more efficient stone erosion in comparison to that applied at high PRF [5]. A similar phenomenon is well documented in SWL, in which testing both *in-vitro* [6–10] and *in-vivo* [11] has shown a decrease in per-shock fragmentation efficiency with increasing shock rate. This is attributed to residual cavitation bubble nuclei that persist from one lithotripsy shock wave (LSW) to the next. While primary cavitation induced by an LSW has been identified as a crucial component of the stone comminution process [4, 12–17], its collapse is typically accompanied by fission into numerous microscopic residual daughter bubbles [18–21] which can persist on the order of a full second [20–23]. It has been shown that LSW propagation through a medium containing these residual daughters induces the selective attenuation of its negative tail [6, 24–26], reducing the energy that ultimately reaches the stone and compromising comminution efficiency. The use of higher shock rates reduces the time available for passive dissolution of residual bubble nuclei between successive LSWs, leading to more pronounced attenuative effects.

Our recent work has aimed to develop a strategy for the active removal of residual bubble nuclei following a cavitation event [27, 28]. We have demonstrated that the application of appropriately designed low-amplitude ultrasound pulses can stimulate the aggregation and subsequent coalescence of a population of residual bubbles, effectively removing them from the field. These pulses—which we term bubble removal pulses—are typically on the order of one millisecond in duration and have maximal nuclei consolidation effects near a mechanical index (MI) of 1 [27, 28]. Previous work has also demonstrated that higher frequency bubble removal pulses (2 MHz) are more effective in comparison to lower frequency (500 kHz) for consolidation of the remnant cavitation nuclei that persist following histotripsy bubble cloud collapse [28]. This is hypothesized to be a result of the secondary Bjerknes force being the major facilitator of the coalescence phenomenon, the attractive magnitude of which is maximized when neighboring bubbles oscillate in-phase with one another [29].

In the present study, we incorporate bubble removal pulses into histotripsy treatment of model kidney stones in an effort to alleviate the rate-dependent efficacy previously observed for histotripsy stone erosion. Cystine-mimicking model stones were sonicated with histotripsy pulses applied at PRFs ranging from 1–500 Hz; at each rate, comminution was quantified with and without the incorporation of bubble removal pulses. It is our hope that this investigation will not only lead to drastic improvements in the efficiency of histotripsy

stone erosion at high PRF, but also serve to expand our understanding regarding the complex role of cavitation in the stone comminution process.

METHODS

A. Model Urinary Stones

Composite stone phantoms formulated to mimic the tensile fracture strength of naturally occurring cystine calculi were cast from a mixture of BegoStone plaster (BEGO USA, Smithfield, RI), albumin (Carolina Biological Supply Co., Burlington, NC), and tap water. Following the methods of Simmons, *et al.* [30] the constituents were mixed with a mass ratio of 73% BegoStone, 24.5% water, and 2.5% albumin in order to achieve the desired stone properties. 0.6 mL aliquots of the resulting slurry were then distributed into the 1 cm diameter cylindrical wells of a Delrin (DuPont, Wilmington, DE) plastic mold and allowed to cure overnight. The next day, stones were removed from the mold and slowly heated to 90°C in a low-temperature oven (Model 10GC, Quincy Lab Inc., Chicago, IL), where they were held for 12 hours to permit albumin polymerization. Finally, stones were allowed to cool back to room temperature and submersed in a beaker of tap water to hydrate. Prior to treatment, phantoms in the hydrated state were degassed overnight in a vacuum desiccator (Bel-Art Products, Wayne, NJ) to minimize any air trapped in the stone material. The end result of this process was the production of cylindrical model stones measuring 1 cm in diameter and having a hydrated mass of 1.01 ± 0.03 g (mean \pm SD, $n = 45$).

B. Experimental Setup

The experimental setup used to study the impact of bubble removal pulse sequences on histotripsy erosion of model kidney stones is displayed in Fig. 1. All experiments were conducted in a water tank measuring $58 \times 43 \times 45$ cm (L \times W \times H), which was filled with deionized water degassed to physiologically relevant levels (dissolved oxygen content of 7.0 ± 0.3 mg/L at 21.2 ± 1.2 °C, corresponding to $77 \pm 3\%$ of saturation); this mimics the dissolved gas content of human urine, for example [31–33]. Dissolved oxygen levels were measured at the beginning and end of each treatment day ($n = 18$) using a Traceable Digital Oxygen Meter (Control Co., Friendswood, TX).

A 500 kHz histotripsy transducer constructed in-house was used to deliver histotripsy therapy to the model stones treated in this study. It consisted of 112 individual watertight modules arranged in a spherical cap pattern with a 150 mm radius of curvature and 270 mm aperture. This geometry was maintained via a scaffold fabricated from Accura 60 plastic (3D Systems Inc., Rock Hill, SC) on a stereolithography machine. Individual module housings were also fabricated from Accura 60 using stereolithography. Within each, two 1-MHz Pz36 disc elements (Ferroperm Piezoceramics A/S, Kvistgaard, Denmark) measuring 20 mm in diameter and 1.6 mm in thickness were stacked and driven in unison to produce a 500-kHz equivalent source. Epoxy adhesive (Hysol E-120 HP, Loctite Corporation, Rocky Hill, CT) was used to bond the individual Pz36 elements together, as well as mate the front face of each stack to a flat Accura-60 disc. The latter served to provide both electrical insulation and acoustic matching between the elements and water. A marine grade epoxy (TAP Epoxy System 314 Resin/143 Hardener, TAP Plastics Inc., San Leandro, CA) was

used to pot the back of each module, ensuring complete electrical insulation from the surrounding water. Overall, this arrangement of 112 modules produced a focal zone having -6 -dB beamwidths measuring 2.0 mm in the lateral dimension and 6.3 mm in the axial. These measurements were conducted at a pressure amplitude of 8 MPa (linear regime) using a fiber optic hydrophone with a 100- μ m-diameter sensing tip [34]. The histotripsy transducer was driven using a pulse amplifier developed in our lab, which was designed to produce very short, intense bursts. More details regarding the acoustic output generated by this setup are provided in the subsequent section.

A separate 1 MHz transducer—which we denote as the bubble removal module—was used to sonicate residual bubble nuclei produced by collapse of the histotripsy bubble cloud. It consisted of a single 1 MHz PZT-4 disc element (Steiner & Martins Inc., Miami, FL) measuring 50 mm in diameter and 2 mm in thickness. This frequency was selected based on our previous observation that bubble removal pulses of higher frequency (>500 kHz) produce more effective consolidation of residual nuclei following histotripsy bubble cloud collapse [28]. Similar to the histotripsy modules, the PZT-4 element was sealed within a stereolithography-fabricated Accura-60 housing. In this case the front face of the housing contained an acoustic lens having a focal length of 175 mm; this design was utilized to center the beam of the bubble removal module coincident with the histotripsy focus when the module was held within a central port in the histotripsy transducer scaffold (Fig. 1). The PZT-4 element was matched to the lens using an epoxy (1C-LV Hysol, Loctite Corporation, Rocky Hill, CT) filled 50 mesh copper screen (McMaster-Carr, Aurora, OH) to achieve the proper thickness and impedance. This arrangement produced an acoustic field with -6 -dB beamwidths measuring 7.0 mm in the lateral dimension and exceeding 100 mm in the axial; as such, the bubble removal field fully encompassed the focal zone generated by the histotripsy transducer. These field scans were performed at a pressure amplitude of 300 kPa (linear regime) using an HNR-0500 needle hydrophone (Onda Corporation, Sunnyvale, CA). The bubble removal module was driven using a 1 MHz sinusoid from an ENI AP400B controllable power amplifier (Electronic Navigation Industries Inc., Rochester, NY); further details on the acoustic output are presented in the subsequent section.

Cystine-mimicking BegoStone cylinders were held within a gel-holder assembly designed to maintain stone position within the focal zone while minimizing attenuation of incident acoustic pulses (Fig. 1). The gel-holder was constructed from Accura 60 plastic and contained a concave pedestal onto which stone phantoms were ultimately placed. An optically transparent 2% agarose hydrogel (LabScientific MB Grade AG-SP, LabScientific Inc., Livingston, NJ) was cast surrounding this pedestal, creating a central channel measuring 15 mm in diameter and 40 mm in height. Stone phantoms were free to move/rotate within the channel during sonication; however, the dimensions were such that the full extent of the histotripsy focal zone was always maintained on the stone surface. As indicated in Fig. 1, the gel-holder assembly was positioned below the histotripsy transducer and stones were sonicated in a top-down orientation. Alignment of the therapy focus to the stone was maintained on an inter-trial basis via two lasers laterally positioned at the known geometric focal location.

C. High-Speed Imaging

High speed images for stone treatments conducted with each parameter set were acquired using a Photron Fastcam SA1.1 high speed camera (Photron USA Inc., San Diego, CA) equipped with a 200 mm macro lens (AF Micro-Nikkor 200mm f/4D IF-ED, Nikon Corporation, Tokyo, Japan). A large-area, high-power LED light source (Bridgelux 50C10K, Bridgelux Inc., Livermore, CA) was used to backlight the experiments such that bubbles generated in the field were visible as dark shadows on the optical images. A 39-frame sequence was recorded immediately following histotripsy pulse firing at a frame rate of 20 kfps and exposure time of 49 μ s, such that the entirety of the acoustic pulse sequence detailed in Fig. 2(c) was imaged.

D. Acoustic Pulse Sequence

Two general types of acoustic pulses were utilized in this study, as represented in Figs. 2(a) and 2(b): 1) Histotripsy pulses generated by the 500 kHz histotripsy transducer were used to initiate a cavitation bubble cloud at the surface of the stone phantom, generating erosion damage consistent with our previous work [1–3]; 2) Bubble removal pulses produced by the 1 MHz bubble removal module were used to sonicate residual nuclei following histotripsy bubble cloud collapse, stimulating their coalescence and removal from the field. The overall timing of this pulse scheme is displayed in Fig. 2(c), with specifics provided henceforth.

Histotripsy pulses used in this study were very short (approximately 5 μ s), had a center frequency of 500 kHz, and an estimated peak-negative pressure (P_-) of 45 MPa. The representative waveform displayed in Fig. 2(a), which was measured using the same fiber optic hydrophone used to perform histotripsy field scans, demonstrates the general shape of a histotripsy pulse. However, it was acquired at a lower P_- of 12 MPa, as calibration at higher amplitudes can result in instantaneous cavitation on the fiber tip. The therapy P_- of 45 MPa reported here was estimated assuming no bubble shielding and using extrapolation based on the observation that P_- increases linearly with the transducer driving voltage.

A partial segment of a representative bubble removal pulse is displayed in Fig. 2(b), acquired using the same HNR-0500 needle hydrophone used to perform bubble removal module field scans. All bubble removal pulses had a center frequency of 1 MHz, duration of 1500 μ s, and amplitude of either 0 (i.e. no bubble removal) or 1 MPa. The latter setting, corresponding to an MI of 1, was selected based on our previous work demonstrating that the efficacy of the bubble removal process peaks near an MI of 1 [28]. Following histotripsy pulse firing, a 500 μ s delay was imposed to allow for unimpeded bubble cloud collapse prior to sonication with the bubble removal pulse. This delay, combined with the fixed 1500 μ s bubble removal pulse duration, limited the maximum investigated histotripsy PRF to 500 Hz. Four PRFs (1, 10, 100, and 500 Hz) were tested to investigate the effect of pulse rate on the efficacy of histotripsy stone erosion.

E. Model Stone Treatment and Damage Quantification

Five model stones were treated with each of the eight parameter combinations investigated in this study. In order to achieve an accurate comparison of stone erosion across all cases, a preliminary investigation was conducted to determine the number of pulses required to

produce similar degrees of damage at each rate. This was deemed preferable to applying treatment for a set time duration or a set number of pulses, as the histotripsy PRFs explored in this study span a 500-fold range and have highly variable comminution outcomes. For example, 10,000 pulses applied at a PRF of 1 Hz (166.7 minutes) may erode nearly the entire model stone, whereas 10,000 pulses applied at a PRF of 500 Hz (20 seconds) may not produce any perceptible damage. For this reason, the following treatment durations were used for each respective PRF in order to produce more similar degrees of stone erosion: (A) PRF= 1 Hz: 2,000 pulses (33.3 minutes); (B) PRF= 10 Hz: 5,000 pulses (8.3 minutes); (C) PRF= 100 Hz: 20,000 pulses (3.3 minutes); (D) PRF= 500 Hz: 50,000 pulses (1.7 minutes).

To quantify the effect of histotripsy erosion, stone mass was measured before and after treatment. These measurements correspond to the hydrated mass of the stone, and care was taken to gently blot any standing water off the stone surface prior to their acquisition. Pre- and post-treatment stone mass was used to quantify both an average treatment rate (mass eroded/treatment time) and average treatment efficiency (mass eroded/number of pulses applied) for a given parameter set.

RESULTS

The erosion efficiency (mg/1000 pulses) and erosion rate (mg/min) resulting from histotripsy treatment of model stones with and without the incorporation of bubble removal pulses are displayed in Fig. 3. Consistent with previous work [1–3], all histotripsy treatments were observed to erode fine particulate debris from the stone surface from the onset of treatment, with no subdivision of the stone into large fragments (à la SWL) ever produced. All treatments generated a statistically significant reduction in stone mass relative to control stones (*t-test*, $P < 0.02$), which were handled in the same manner as treated stones but not exposed to ultrasound. The treatment parameters utilized in this study resulted in only partial erosion of model stones, as is exemplified in Fig. 4.

Without the incorporation of bubble removal, the efficiency of histotripsy stone erosion (Fig. 3, top panel) displayed an extreme dependence on PRF. Maximum efficiency was achieved for the lowest tested PRF of 1 Hz, which eroded 23.4 ± 6.2 mg/1000 pulses. All higher PRFs showed a significant drop in efficiency relative to this value (*t-test*, $P < 0.0001$). Specifically, application of histotripsy at 10 Hz resulted in an efficiency reduction to 2.8 ± 1.7 mg/1000 pulses. PRFs of 100 and 500 Hz produced efficiencies of 0.5 ± 0.1 and 0.4 ± 0.2 mg/1000 pulses, which were not statistically different from one another (*t-test*, $P = 0.45$). Alternatively, the erosion characteristics resulting from histotripsy treatment can be expressed as a temporal rate (Fig. 3, lower panel). In this case the rate of histotripsy stone erosion is observed to reach a maximum of 11.3 ± 6.9 mg/min at the highest tested PRF of 500 Hz (*t-test*, $P < 0.03$). Treatment at the lower PRFs of 1, 10, and 100 Hz produced erosion rates of 1.4 ± 0.4 , 1.7 ± 1.0 , and 2.8 ± 0.7 mg/min, respectively. Clearly, a 10-fold increase in PRF does not translate to a 10-fold increase in rate of erosion.

The incorporation of bubble removal pulses resulted in drastic enhancement of histotripsy stone erosion for PRFs of 10 Hz and above. At the lowest tested PRF of 1 Hz—in which case residual bubble nuclei had a full second for passive dissolution—a statistically

significant difference in erosion was not observed in comparing histotripsy only vs. histotripsy with bubble removal (*t-test*, $P = 0.17$). At all PRFs above 1 Hz, however, the addition of bubble removal pulses produced a significant increase in erosion relative to their histotripsy-only counterpart (*t-test*, $P < 0.015$). Specifically, at PRFs of 10, 100, and 500 Hz erosion (both efficiency and rate) increased 3.7-, 7.5-, and 2.7-fold. Fig. 4 shows the outcome of the five stone erosion trials performed at a PRF of 100 Hz without (top panel) and with (bottom panel) bubble removal. In each case stone material was eroded from the surface in the region targeted by the histotripsy focus; however, the incorporation of bubble removal pulses allowed for an average erosion rate of 21.1 mg/min over the 3.3 minute treatment time, in comparison to the 2.8 mg/min rate produced by histotripsy in isolation.

Representative high speed images showing histotripsy bubble cloud dynamics for low PRF (1 Hz) and high PRF (100 Hz) treatments are displayed in Fig. 5. Each image sequence corresponds to the 100th pulse in a series applied at each respective rate, with $t = 0 \mu\text{s}$ indicating the time of pulse arrival at the stone. At the low rate of 1 Hz, bubble cloud dynamics are extremely similar across the histotripsy-only (Fig. 5, top panel, upper row) and histotripsy with bubble removal (Fig. 5, top panel, lower row) cases. In each, prefocal cavitation upon histotripsy pulse arrival is minimal and cloud collapse occurs as a coherent unit against the stone surface 200–250 μs following initiation. Cloud dynamics at the high PRF of 100 Hz display markedly different characteristics when no bubble removal pulses are applied (Fig. 5, bottom panel, upper row). In this case, prefocal cavitation upon histotripsy pulse arrival is much more extensive, and the bubble cloud displays a shorter lifetime collapsing in the time window of 150–200 μs . Furthermore, cloud collapse appears more disparate rather than a cohesive unit, and the final collapse point resides prefocal to the stone surface (seen in the frame at 150 μs , arrow). Incorporation of bubble removal pulses in histotripsy applied at a PRF of 100 Hz results in cloud dynamics more closely approximating those observed at 1 Hz (Fig. 5, bottom panel, lower row). Here, the extent of prefocal cavitation upon histotripsy pulse arrival is greatly reduced relative to the case of 100 Hz without bubble removal, although some bubble excitation is still observed in the periphery. The lifetime of the cloud is roughly 200 μs , falling in a range intermediate to that for 100 Hz without bubble removal and the 1 Hz cases. Finally, the ultimate point of cloud collapse resumes its position adjacent to the stone surface (as seen in the frame at 200 μs). [Note: This paper has supplementary downloadable material available at <http://ieeexplore.ieee.org>, provided by the authors. This includes the full video sequences corresponding to the image sets displayed in Fig. 5. All videos were taken at 20 kfps with a 49 μs exposure, and show the entire duration of the experimental pulse sequence displayed in Fig. 2(c).]

DISCUSSION

This study demonstrates a unique strategy for mitigating the rate-limiting effects of residual bubble nuclei in histotripsy kidney stone erosion, using low-amplitude ultrasound pulses to stimulate their removal from the field via bubble coalescence. When histotripsy is applied in isolation, the efficiency of stone erosion displays a precipitous drop-off for tested PRFs above 1 Hz. This is likely a result of the remnant bubble nuclei produced by primary cavitation collapse persisting on the order of one second [20–23]; as such, the lowest tested

rate of 1 Hz is expected to afford the majority of residual bubbles sufficient time for passive dissolution between histotripsy pulses. Further support for this idea is offered by the observation that introducing bubble removal pulses did not produce a statistically different outcome in erosion at this lowest tested PRF. Contrastingly, at PRFs of 10 Hz and above the incorporation of bubble removal in histotripsy therapy resulted in pronounced improvements in erosion efficiency. At 10, 100, and 500 Hz, the extent of erosion was observed to increase 3.7-, 7.5-, and 2.7-fold relative to the respective histotripsy-only cases.

The bubble removal strategy used in this study has been introduced previously [27, 28], and is thought to achieve the aggregation and subsequent coalescence of residual bubble nuclei through an interplay of the Bjerknes forces. Our preliminary work has suggested that it is the secondary Bjerknes force that is the major contributor to this bubble consolidation phenomenon, with this dominance manifesting in higher bubble removal frequencies producing enhanced nuclei consolidation effects [28]. Although not yet fully optimized, the 1 MHz bubble removal pulse scheme utilized in this study represents a compromise between the use of high frequency to maximize bubble aggregation and focal volume size to cover the region of interest. One of the practical limitations in moving to higher frequency is a reduction in focal coverage. Here, the 1 MHz bubble removal module produced a focal zone with a -6 -dB beamwidth measuring 7.0 mm in the lateral direction. While this is certainly large enough to encompass the 2.0 mm -6 -dB lateral beamwidth of the histotripsy transducer, it is possible that some residual bubble nuclei could escape to the periphery of the 15 mm diameter treatment channel. This is especially possible at the higher PRFs tested in this study, which are expected to generate some degree of fluid flow within the treatment channel. As such, one possible explanation for the failure of bubble removal pulses to achieve complete recovery of erosion efficiency is the persistence of residual nuclei outside the bubble removal focus. Evidence of this can be observed in the first frame corresponding to a PRF of 100 Hz with bubble removal in Fig. 5.

The trends in histotripsy stone erosion observed in this study are consistent with previous work in the field of SWL, which has implicated residual bubble nuclei as the primary contributor to the rate-dependent efficacy observed for stone comminution. Extensive testing has documented that LSWs applied at low rate produce a greater per-shock fragmentation efficiency in comparison to those applied at high rate [6–11]. These results are corroborated by an abundance of clinical data [35–41], which indicates that SWL performed at shock rates of 1–1.5 Hz produces more successful treatment outcomes than that at 2 Hz. It is the persistence of residual cavitation nuclei between successive LSWs that is responsible for these effects. While the lifespan of primary cavitation bubbles generated by an LSW is only on the order of 1 ms [42–45], their collapse has been shown to generate a large population of residual daughter bubbles—i.e. cavitation nuclei—that can persist on the order of 1 second [20–23]. When an LSW propagates through a medium containing these residual bubbles the tensile component of the waveform will cause them to grow, effectively removing energy from the LSW and leaving it behind in the form of kinetic and potential energy of the fluid surrounding the bubbles [25]. As such, the remnant nuclei induce the selective attenuation of an LSW's negative tail [6, 24–26] and reduce the energy that ultimately reaches the targeted stone, compromising comminution efficiency.

While the population of cavitation bubbles generated by an LSW is certainly different from a histotripsy bubble cloud, the ill-effects of residual cavitation nuclei experienced in SWL extend to histotripsy stone erosion therapy. Previous work has shown that the collapse of a histotripsy bubble cloud produces an extensive set of microscopic residual daughter bubbles [27, 46, 47]. Furthermore, propagation of an acoustic pulse through this population of remnant bubbles was observed to experience pronounced attenuation as measured by a hydrophone positioned distal to the histotripsy focus [28]. Similar to SWL, the expansion of remnant bubble nuclei induced by the histotripsy pulse will detract energy from the pulse directly; the expanded bubbles are likely to then provide a larger area for further scattering of the remainder of the histotripsy pulse. It is likely that the resulting pulse attenuation is partially responsible for the decreased efficiency of stone erosion observed at high PRF. Indeed, as represented in Fig. 5 the lifetime of histotripsy bubble clouds generated at high PRF was reduced relative to those produced at low PRF, suggesting a reduction in the pulse energy reaching the focal point in these cases.

A second major implication of residual bubble nuclei in histotripsy stone erosion is their influence on the location of bubble cloud collapse. As represented by the case of 100 Hz without bubble removal in Fig. 5, the point of cloud collapse was consistently observed to shift prefocal to the stone surface when high PRFs were utilized. Conversely, at the lowest tested PRF of 1 Hz the bubble cloud collapsed as a coherent unit against the stone surface with each histotripsy pulse applied. This suggests that remnant nuclei that persist in the field act to seed the point of cloud collapse away from the stone. A similar result was observed by Chitnis, *et al.* [48], who found that bubble clouds generated near a clean ceramic face collapsed onto the boundary; however, when the ceramic face contained a sparse bubble layer, cloud collapse shifted away from the surface and cavitation damage was mitigated. To the best of the authors' knowledge this phenomenon has not been observed with respect to the effect of remnant bubble nuclei in SWL. Nevertheless, it appears to be an extremely important feature of efficient erosion in histotripsy therapy. The incorporation of bubble removal pulses facilitated the recovery of the collapse point toward the stone surface when high PRFs were utilized.

While the bubble removal pulses utilized in this study have not yet been fully optimized, they serve to demonstrate the drastic impact that residual cavitation nuclei can have on histotripsy kidney stone erosion. Furthermore, this strategy provides us with a tool through which we can begin to identify the aspects of histotripsy-induced cavitation that are crucial for the efficient erosion of a targeted structure. The results of this study suggest that, through appropriate manipulation of the cavitation environment surrounding the stone, the erosion efficiency achieved at low pulse rates can be recovered when high PRFs are utilized. It is important to note that these results were obtained in a simplified *in-vitro* setting, and our future work will focus on translating this approach to the more complex environment *in-vivo*. It is our hope that the treatment rates afforded by an optimized form of this bubble removal strategy will allow histotripsy stone erosion to offer a viable adjunct to SWL procedures.

CONCLUSION

Similar to SWL, histotripsy treatment of model kidney stones displays a rate-dependent efficacy in which pulses applied at low PRF achieve drastically higher erosion efficiency in comparison to those applied at high PRF. This is attributed to residual cavitation bubble nuclei that are generated by histotripsy bubble cloud collapse and persist from one pulse to the next. Such residual bubbles can cause direct attenuation of the incident acoustic waveform, as well as influence the resulting cavitation dynamics—seeding collapse of the bubble cloud prefocal to the targeted stone surface. The most direct approach to mitigating the effects of remnant bubbles is to simply wait long enough for their passive dissolution between successive pulses. While this may afford a high per-pulse efficiency, the temporal rate of stone erosion suffers. It is for this reason that we have developed an active means of bubble removal, using low-amplitude acoustic pulses to stimulate the aggregation and subsequent coalescence of residual nuclei. Although not yet fully optimized, the results of this study suggest that these bubble removal pulses offer great promise in recovering high per-pulse efficiency when high PRFs are utilized. The continued development of this approach will offer further insight into the qualities of cavitation that are paramount to effective stone comminution, while successful translation to an *in-vivo* model stands to drastically enhance the efficacy of histotripsy for the application of kidney stone treatment.

Supplementary Material

Refer to Web version on PubMed Central for supplementary material.

ACKNOWLEDGMENTS

Research reported in this publication was supported by The National Institute of Diabetes and Digestive and Kidney Diseases of the National Institutes of Health under award number R01DK091267. The content is solely the responsibility of the authors and does not necessarily represent the official views of the National Institutes of Health.

REFERENCES

1. Duryea AP, Hall TL, Maxwell AD, Xu Z, Cain CA, Roberts WW. Histotripsy erosion of model urinary calculi. *J Endourol.* 2011 Feb;25:341–344. [PubMed: 21091223]
2. Duryea AP, Maxwell AD, Roberts WW, Xu Z, Hall TL, Cain CA. In vitro comminution of model renal calculi using histotripsy. *IEEE Trans Ultrason Ferroelectr Freq Control.* 2011 May;58:971–980. [PubMed: 21622053]
3. Duryea AP, Roberts WW, Cain CA, Hall TL. Controlled cavitation to augment SWL stone comminution: mechanistic insights in vitro. *IEEE Trans Ultrason Ferroelectr Freq Control.* 2013 Feb;60:301–309. [PubMed: 23357904]
4. Zhu S, Cocks FH, Preminger GM, Zhong P. The role of stress waves and cavitation in stone comminution in shock wave lithotripsy. *Ultrasound Med Biol.* 2002 May;28:661–671. [PubMed: 12079703]
5. Duryea, AP.; Roberts, WW.; Cain, CA.; Hall, TL. Optimization of histotripsy for kidney stone erosion; *Ultrasonics Symposium (IUS), 2010 IEEE*; 2010. p. 342-345.
6. Pishchalnikov YA, McAteer JA, Williams JC Jr, Pishchalnikova IV, Vonderhaar RJ. Why stones break better at slow shockwave rates than at fast rates: in vitro study with a research electrohydraulic lithotripter. *J Endourol.* 2006 Aug;20:537–541. [PubMed: 16903810]

7. Vallancien G, Munoz R, Borghi M, Veillon B, Brisset JM, Daudon M. Relationship between the frequency of piezoelectric shock waves and the quality of renal stone fragmentation. In vitro study and clinical implications. *Eur Urol.* 1989; 16:41–44. [PubMed: 2714316]
8. Wiksell H, Kinn AC. Implications of cavitation phenomena for shot intervals in extracorporeal shock wave lithotripsy. *Br J Urol.* 1995 Jun.75:720–723. [PubMed: 7613826]
9. Greenstein A, Matzkin H. Does the rate of extracorporeal shock wave delivery affect stone fragmentation? *Urology.* 1999; 54:430–432. [PubMed: 10475348]
10. Weir MJ, Tariq N, Honey RJ. Shockwave frequency affects fragmentation in a kidney stone model. *J Endourol.* 2000 Sep.14:547–550. [PubMed: 11030533]
11. Paterson RF, Lifshitz DA, Lingeman JE, Evan AP, Connors BA, Fineberg NS, et al. Stone fragmentation during shock wave lithotripsy is improved by slowing the shock wave rate: studies with a new animal model. *J Urol.* 2002 Nov.168:2211–2215. [PubMed: 12394761]
12. Delius M, Brendel W, Heine G. A mechanism of gallstone destruction by extracorporeal shock waves. *Naturwissenschaften.* 1988 Apr.75:200–201. [PubMed: 3398924]
13. Bailey MR. Control of Acoustic Cavitation with Application to Lithotripsy. DTIC Document. 1997
14. Vakil N, Everbach EC. Transient acoustic cavitation in gallstone fragmentation: A study of gallstones fragmented *in vivo*. *Ultrasound in medicine & biology.* 1993; 19:331–342. [PubMed: 8346607]
15. Delius M. Minimal static excess pressure minimises the effect of extracorporeal shock waves on cells and reduces it on gallstones. *Ultrasound in Medicine & Biology.* 1997; 23:611–617. // [PubMed: 9232770]
16. Bailey MR, Cleveland RO, Colonius T, Crum LA, Evan AP, Lingeman JE, et al. Cavitation in shock wave lithotripsy: the critical role of bubble activity in stone breakage and kidney trauma. *Ultrasonics 2003 IEEE Symposium on.* 2003; 1:724–727.
17. Xi X, Zhong P. Improvement of stone fragmentation during shock-wave lithotripsy using a combined EH/PEAA shock-wave generator—in vitro experiments. *Ultrasound in Medicine & Biology.* 2000; 26:457–467. 3//. [PubMed: 10773377]
18. Flynn HG, Church CC. A mechanism for the generation of cavitation maxima by pulsed ultrasound. *J Acoust Soc Am.* 1984 Aug.76:505–512. [PubMed: 6481000]
19. Brennen CE. Fission of collapsing cavitation bubbles. *Journal of Fluid Mechanics.* 2002; 472:153–166.
20. Pishchalnikov, YA.; McAteer, JA.; Pishchalnikova, IV.; Williams, JC.; Bailey, MR.; Sapozhnikov, OA. Bubble proliferation in shock wave lithotripsy occurs during inertial collapse; 18th International Symposium on Nonlinear Acoustics; 2008. p. 460-463.
21. Pishchalnikov YA, Williams JC, McAteer JA. Bubble proliferation in the cavitation field of a shock wave lithotripter. *J Acoust Soc Am.* 2011 Aug.130:EL87–EL93. [PubMed: 21877776]
22. Huber P, Jochle K, Debus J. Influence of shock wave pressure amplitude and pulse repetition frequency on the lifespan, size and number of transient cavities in the field of an electromagnetic lithotripter. *Phys Med Biol.* 1998 Oct.43:3113–3128. [PubMed: 9814538]
23. Epstein PS, Plesset MS. On the stability of gas bubbles in liquid-gas solutions. *The Journal of Chemical Physics.* 1950; 18:1505–1509.
24. Pishchalnikov YA, McAteer JA, Williams JC Jr. Effect of firing rate on the performance of shock wave lithotripters. *BJU Int.* 2008 Dec.102:1681–1686. [PubMed: 18710450]
25. Pishchalnikov YA, Sapozhnikov OA, Bailey MR, Pishchalnikova IV, Williams JC, McAteer JA. Cavitation selectively reduces the negative-pressure phase of lithotripter shock pulses. *Acoust Res Lett Online.* 2005 Nov 3.6:280–286. [PubMed: 19756170]
26. Pishchalnikov, YA.; McAteer, JA.; Bailey, MR.; Pishchalnikova, IV.; Williams, JC.; Evan, AP. Acoustic shielding by cavitation bubbles in shock wave lithotripsy (SWL); 17th International Symposium on Nonlinear Acoustics; 2005. p. 319-322.
27. Duryea AP, Cain CA, Tamaddoni HA, Roberts WW, Hall TL. Removal of Residual Nuclei Following a Cavitation Event using Low-Amplitude Ultrasound. *IEEE Trans Ultrason Ferroelectr Freq Control.* 2014 Oct.61:1619–1626. [PubMed: 25265172]

28. Duryea AP, Tamaddoni HA, Cain CA, Roberts WW, Hall TL. Removal of residual nuclei following a cavitation event: a parametric study. *IEEE Trans Ultrason Ferroelectr Freq Control*. Accepted with Minor Revisions.
29. Leighton, TG. *The Acoustic Bubble*. San Diego, CA: Academic Press Inc; 1997.
30. Simmons WN, Cocks FH, Zhong P, Preminger G. A composite kidney stone phantom with mechanical properties controllable over the range of human kidney stones. *J Mech Behav Biomed Mater*. 2010 Jan.3:130–133. [PubMed: 19878912]
31. Chaigneau M, Le Moan G. On the composition of gas dissolved in human urine. *C R Acad Sci Hebd Seances Acad Sci D*. 1968 Nov 25.267:1893–1895. [PubMed: 4973654]
32. Fowlkes JB, Carson PL, Chiang EH, Rubin JM. Acoustic generation of bubbles in excised canine urinary bladders. *J Acoust Soc Am*. 1991 Jun.89:2740–2744. [PubMed: 1918622]
33. Hwang EY, Fowlkes JB, Carson PL. Variables controlling contrast generation in a urinary bladder model. *J Acoust Soc Am*. 1998 Jun.103:3706–3716. [PubMed: 9637051]
34. Parsons JE, Cain CA, Fowlkes JB. Cost-effective assembly of a basic fiber-optic hydrophone for measurement of high-amplitude therapeutic ultrasound fields. *J Acoust Soc Am*. 2006 Mar. 119:1432–1440. [PubMed: 16583887]
35. Madbouly K, El-Tiraifi AM, Seida M, El-Faqih SR, Atassi R, Talic RF. Slow versus fast shock wave lithotripsy rate for urolithiasis: a prospective randomized study. *J Urol*. 2005 Jan.173:127–130. [PubMed: 15592053]
36. Yilmaz E, Batislam E, Basar M, Tuglu D, Mert C, Basar H. Optimal frequency in extracorporeal shock wave lithotripsy: prospective randomized study. *Urology*. 2005 Dec.66:1160–1164. [PubMed: 16360432]
37. Pace KT, Ghiculete D, Harju M. Shock wave lithotripsy at 60 or 120 shocks per minute: A randomized, double-blind trial. *The Journal of Urology*. 2005; 174:595–599. [PubMed: 16006908]
38. Chacko J, Moore M, Sankey N, Chandhoke PS. Does a slower treatment rate impact the efficacy of extracorporeal shock wave lithotripsy for solitary kidney or ureteral stones? *J Urol*. 2006; 175:1370–1373. [PubMed: 16515999]
39. Kato Y, Yamaguchi S, Hori J, Okuyama M, Kakizaki H. Improvement of stone comminution by slow delivery rate of shock waves in extracorporeal lithotripsy. *Int J Urol*. 2006 Dec.13:1461–1465. [PubMed: 17118017]
40. Weiland D, Lee C, Ugarte R, Monga M. Impact of shockwave coupling on efficacy of extracorporeal shockwave lithotripsy. *J Endourol*. 2007 Feb.21:137–140. [PubMed: 17338608]
41. Semins MJ, Trock BJ, Matlaga BR. The effect of shock wave rate on the outcome of shock wave lithotripsy: a meta-analysis. *J Urol*. 2008 Jan.179:194–197. discussion 197. [PubMed: 18001796]
42. Sass W, Dreyer HP, Kettermann S, Seifert J. The role of cavitation activity in fragmentation processes by lithotripters. *J Stone Dis*. 1992 Jul.4:193–207. [PubMed: 10147666]
43. Zhong P, Cioanta I, Cocks FH, Preminger GM. Inertial cavitation and associated acoustic emission produced during electrohydraulic shock wave lithotripsy. *J Acoust Soc Am*. 1997 May.101:2940–2950. [PubMed: 9165740]
44. Zhong P, Tong HL, Cocks FH, Preminger GM. Transient oscillation of cavitation bubbles near stone surface during electrohydraulic lithotripsy. *J Endourol*. 1997 Feb.11:55–61. [PubMed: 9048300]
45. Cleveland RO, Sapozhnikov OA, Bailey MR, Crum LA. A dual passive cavitation detector for localized detection of lithotripsy-induced cavitation in vitro. *J Acoust Soc Am*. 2000 Mar. 107:1745–1758. [PubMed: 10738826]
46. Xu Z, Hall TL, Fowlkes JB, Cain CA. Optical and acoustic monitoring of bubble cloud dynamics at a tissue-fluid interface in ultrasound tissue erosion. *The Journal of the Acoustical Society of America*. 2007; 121:2421–2430. [PubMed: 17471753]
47. Wang TY, Xu Z, Hall TL, Fowlkes JB, Cain CA. An efficient treatment strategy for histotripsy by removing cavitation memory. *Ultrasound Med Biol*. 2012 May.38:753–766. [PubMed: 22402025]
48. Chitnis PV, Manzi NJ, Cleveland RO, Roy RA, Holt RG. Mitigation of damage to solid surfaces from the collapse of cavitation bubble clouds. *Journal of Fluids Engineering*. 2010; 132:051303.

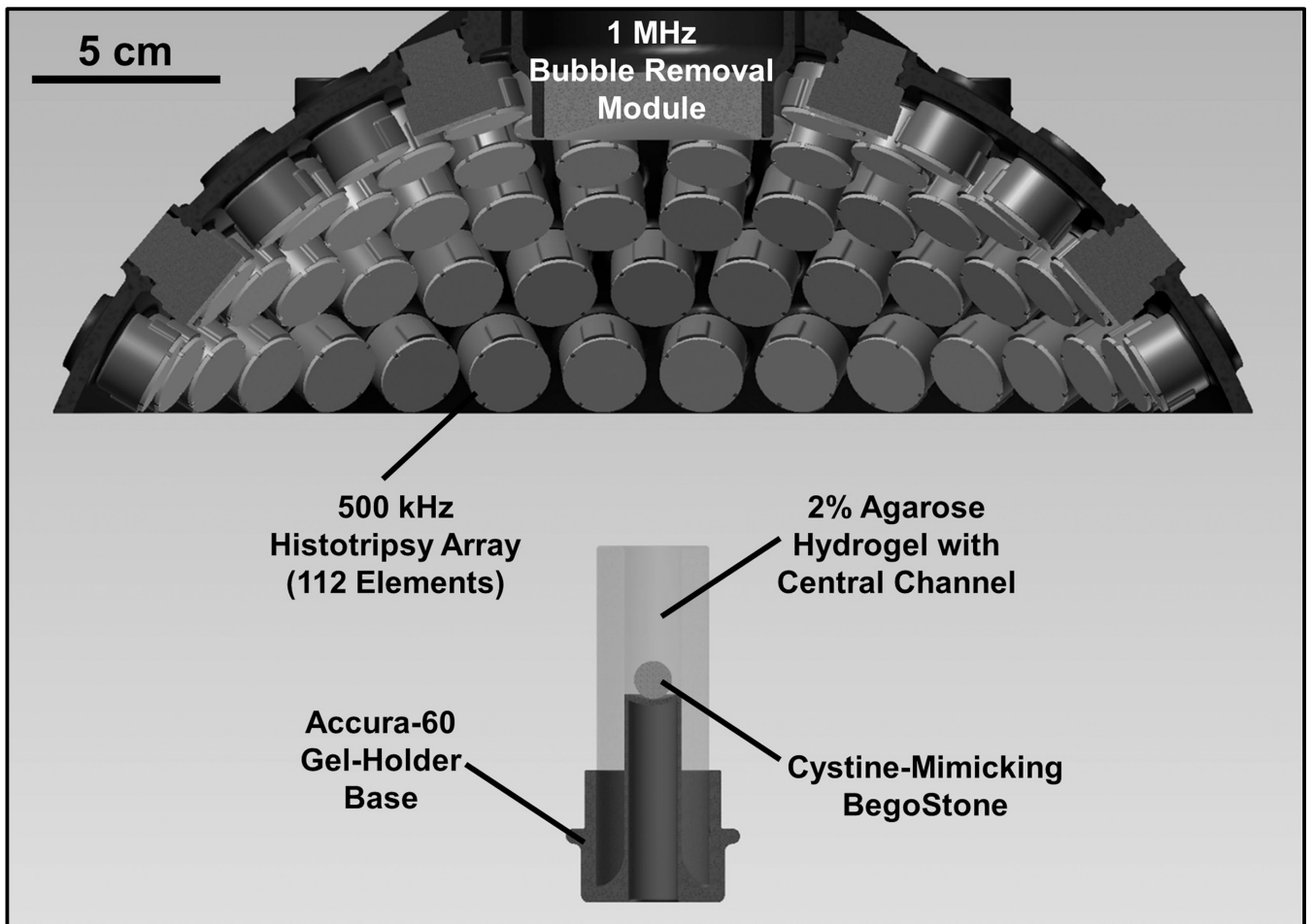


Fig. 1. Experimental setup used to study the effect of bubble removal pulses on histotripsy erosion of model kidney stones. Histotripsy treatment was delivered from a transducer composed of 112 individual 500 kHz modules arranged in a spherical cap pattern, while a separate 1 MHz transducer aligned confocally with the histotripsy array was used to generate bubble removal pulses. Cystine-mimicking BegoStones were positioned within an agarose hydrogel holder for treatment; this assembly was placed below the transducer such that sonication was performed in a top-down orientation.

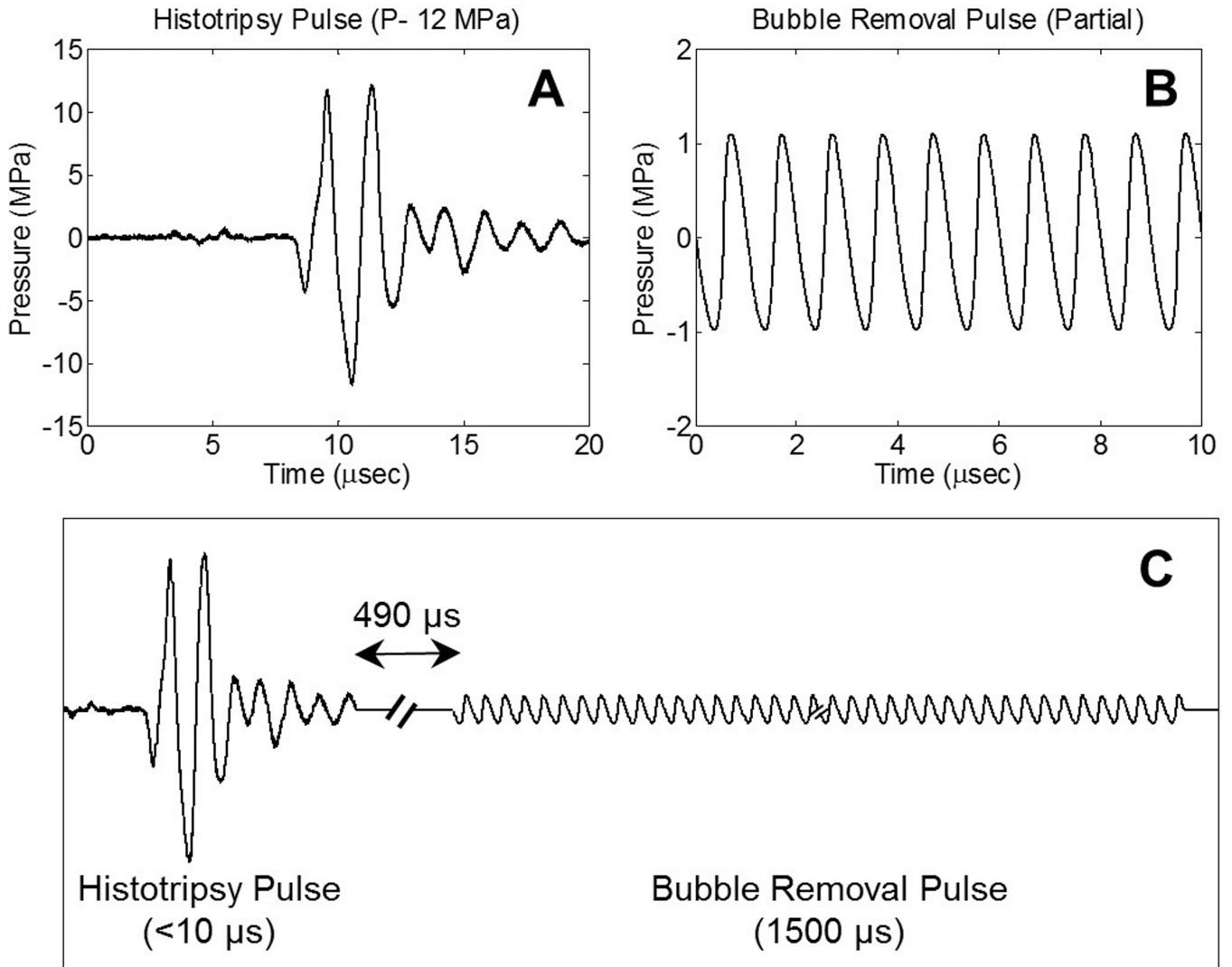


Fig. 2. General pulse scheme used to study the effect of bubble removal pulses on histotripsy erosion of model kidney stones. (a) Representative waveform acquired from the 500 kHz histotripsy transducer at low power (below the cavitation threshold). The histotripsy pulse P- used for stone treatments is estimated to be 45 MPa. (b) Partial segment of the 1500 μs bubble removal pulse; all bubble removal pulses had a center frequency of 1 MHz, and MI set to either 0 or 1. (c) Overall timing of the experimental pulse scheme. A 500 μs delay was imposed following histotripsy pulse firing to allow the bubble cloud to collapse in an unimpeded manner.

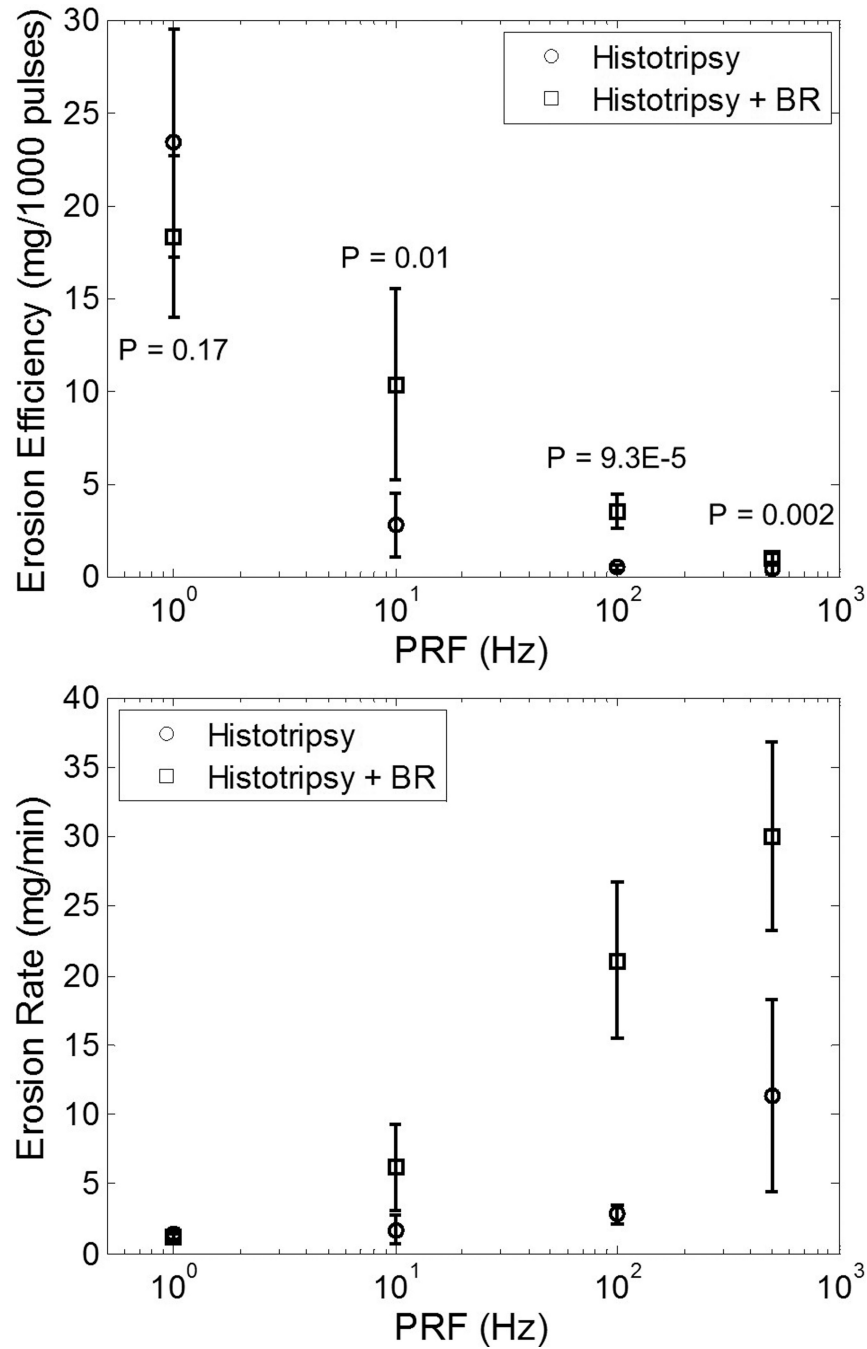


Fig. 3. Erosion efficiency (top panel) and erosion rate (bottom panel) resulting from histotripsy treatment of model stones without and with the incorporation of bubble removal (BR) pulses. Maximum erosion efficiency was produced at the lowest tested PRF of 1 Hz, while the highest rate of erosion was generated at the highest tested PRF of 500 Hz; a 10-fold increase in PRF does not correspond to a 10-fold increase in erosion rate, however. The introduction of bubble removal pulses resulted in a drastic enhancement in erosion for PRFs of 10 Hz and above. This is indicated by the displayed P-values, which show the results of a

t-test between trials without and trials with bubble removal at a given PRF. These P-values are the same whether results are evaluated as erosion efficiency or erosion rate, and as such only displayed on the top panel.

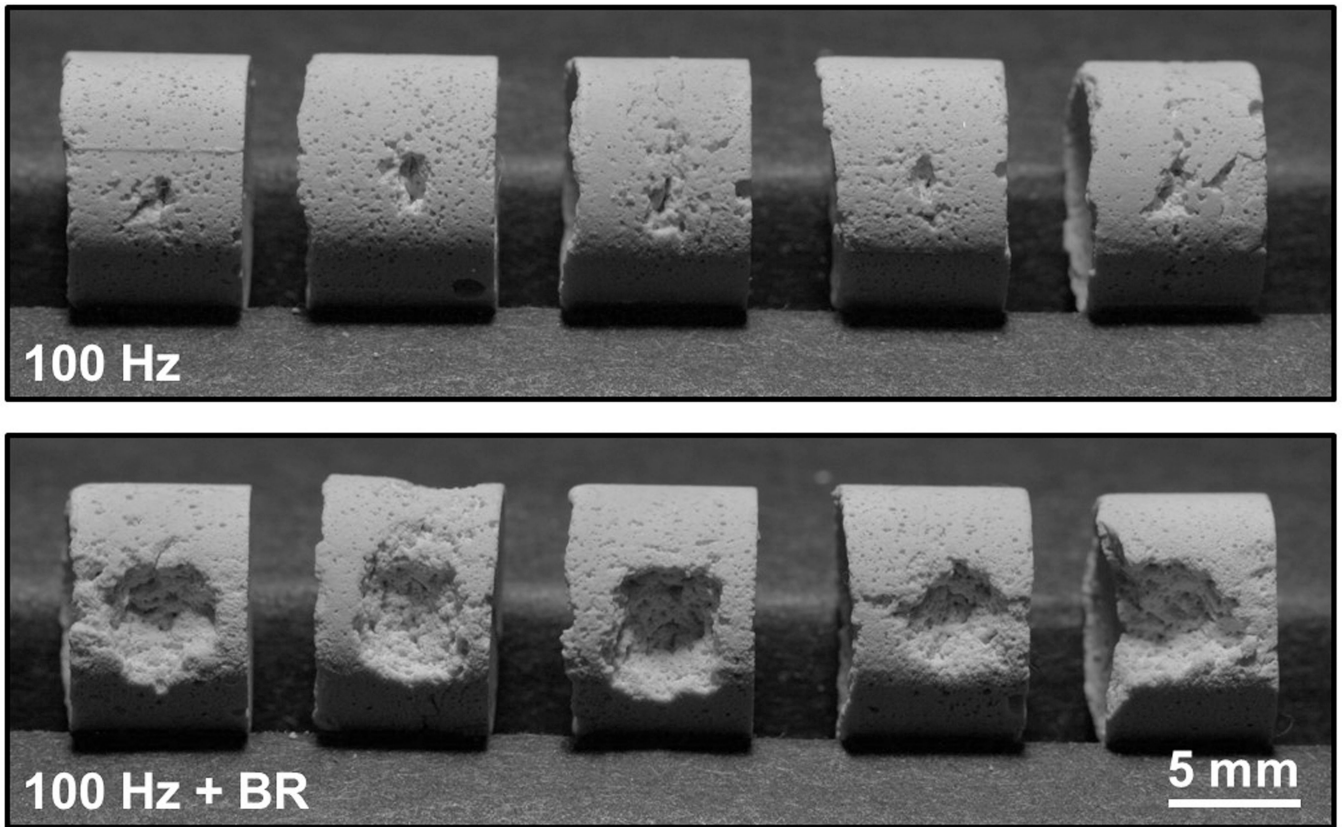


Fig. 4.

Results of five trials performed for histotripsy stone erosion at 100 Hz PRF without (top panel) and with (bottom panel) the incorporation of bubble removal (BR) pulses. In each case material was eroded from the surface of the stone in the region targeted by the histotripsy focus. However, the introduction of bubble removal pulses allowed for an erosion rate of 21.1 ± 5.6 mg/min over the 3.3 minute treatment duration, in comparison to 2.8 ± 0.7 mg/min for histotripsy-only.

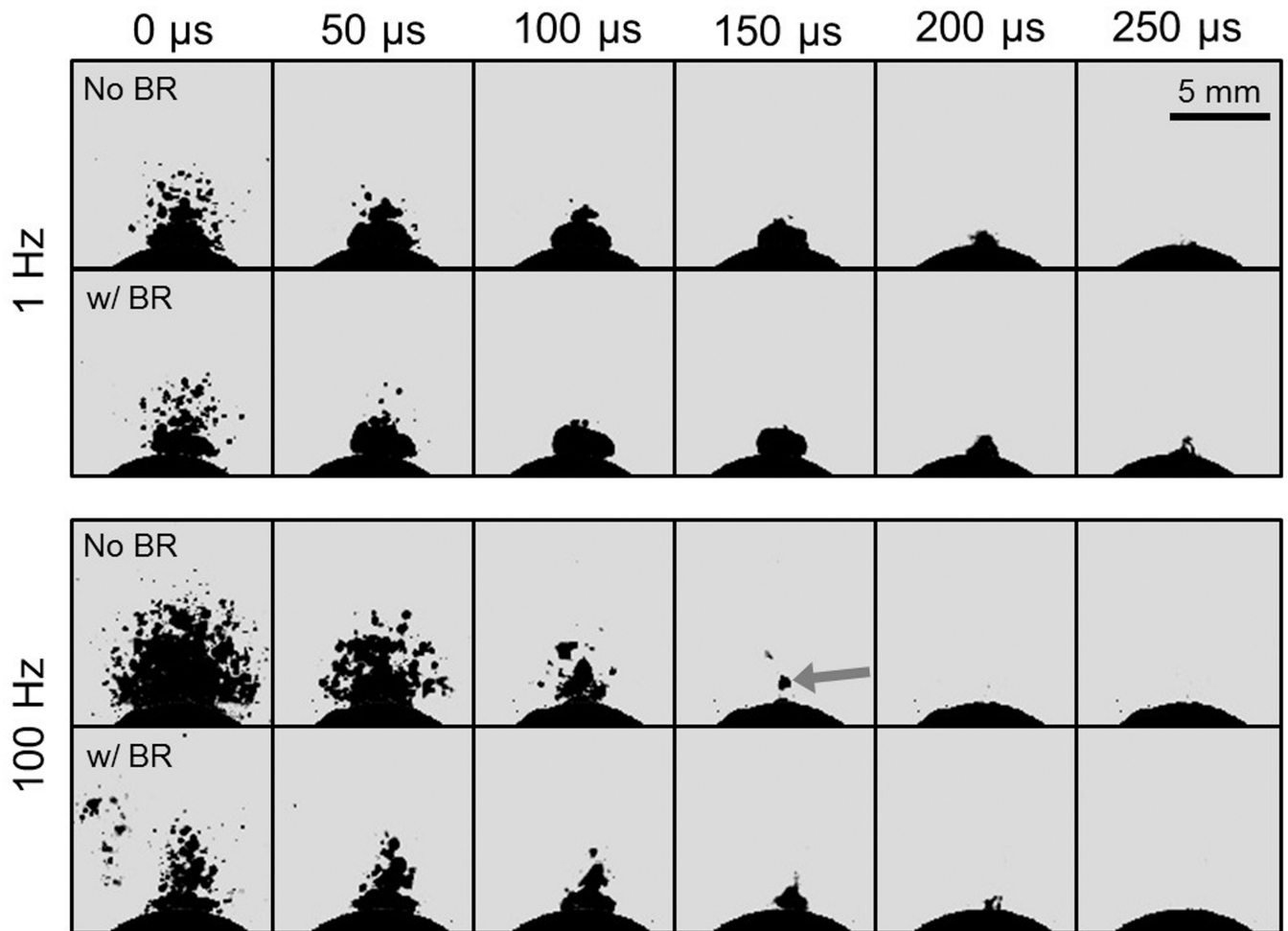


Fig. 5.

Histotripsy bubble cloud dynamics at PRFs of 1 and 100 Hz. Each sequence corresponds to the 100th histotripsy pulse in a series, with $t = 0 \mu\text{s}$ indicating the time at which the pulse arrives at the stone. Each frame was exposed for $49 \mu\text{s}$. For a given PRF, the top row of images displays the bubble cloud time-course for the histotripsy-only case, whereas the bottom row of images shows the cloud dynamics when bubble removal (BR) pulses are incorporated. In the absence of bubble removal, histotripsy applied at the high PRF of 100 Hz generates enhanced prefocal cavitation, reduction of the bubble cloud lifespan, and translation of the point of cloud collapse to a location above the stone (see arrow).